Semi-analytical Modeling of Transition Metal Dichalcogenide (TMD)-based Tunneling Field-effect Transistors (TFETs)

In Huh
Department of Electronic Engineering, Sogang University, 35 Baekbeom-ro, Mapo-gu, Seoul, Korea
E-mail: high_sky_up@naver.com

In this paper, the physics-based analytical model of transition metal dichalcogenide (TMD)-based double-gate (DG) tunneling field-effect transistors (TFETs) is proposed. The proposed model is derived by using the two-dimensional (2-D) Landauer formula and the Wentzel-Kramers-Brillouin (WKB) approximation. For improving the accuracy, nonlinear and continuous lateral energy band profile is applied to the model. 2-D density of states (DOS) and two-band effective Hamiltonian for TMD materials are also used in order to consider the 2-D nature of TMD-based TFETs. The model is validated by using the tight-binding non-equilibrium Green's function (NEGF)-based quantum transport simulation in the case of monolayer molybdenum disulfide (MoS_2)-based TFETs.

I. INTRODUCTION

Recently, tunneling field-effect transistors (TFETs) are considered as one of the most promising candidates for low-power applications thanks to their low off-current (I_{off}) and small subthreshold swing (SS) [1]–[3]. However, some published studies reported that TFETs are difficult to achieve suppressed I_{off} and steep switching characteristics as expected because of the gradual energy band profile at the source/channel tunneling junction [4], [5]. Even if the uniform and abrupt doping profile can be implemented, the fundamental "potential decay rate" is still existed at the tunneling junction. According to the well-known screening length theory proposed by Yan *et al.* [6], the channel screening length (λ_{ch}) determines the potential decay rate at the tunneling junction: As λ_{ch} decreases, TFETs can achieve steeper junction band profile. Therefore, in order to draw the ideal performance of TFETs, λ_{ch} should be scaled down aggressively. In this context, two-dimensional (2-D) transition metal dichalcogenide (TMD) semiconductors have been studied intensively [7]–[9]. It is due to their atomically-thin layer thickness and low permittivity, which result in smaller λ_{ch} than three-dimensional (3-D) semiconductor-based TFETs. For example, λ_{ch} of molybdenum disulfide (MoS_2)-based double-gate (DG) TFETs can be lowered below 5 Å [8].

In order to evaluate the electrical characteristics of TMD-based TFETs, the 2-D band-to-band tunneling current should be modeled accurately. However, rigorous modeling of the 2-D band-to-band tunneling current has not been performed to date. Although Ma *et al* introduce a simple analytical expression for the band-to-band tunneling in 2-D crystal semiconductors [10], it focuses on the physical understanding of 2-D tunneling transport rather than the accurate prediction of TMD-based TFETs' performance. In order to address this problem, in this paper, the 2-D band-to-band tunneling current of TMD-based DG TFETs is modeled carefully. The model is based on the 2-D Landauer formula and the Wentzel-Kramers-Brillouin (WKB) approximation. For improving the accuracy of the modeling, nonlinear and continuous lateral energy band profile is applied to the WKB approximation. Furthermore, 2-D density of states (DOS) and two-band effective Hamiltonian for TMD materials are used in order to cover the 2-D nature of TMD-based TFETs. Modeling results are compared with tight binding non-equilibrium Green's function (NEGF)-based simulation results in the case of monolayer MoS_2-based TFETs.

II. ANALYTICAL MODELING

Fig. 1 shows the schematic of TMD-based DG TFETs. L_{ch}, x_{sj}, t_{ch} and t_{ox} in Fig. 1 represent the channel length, position of the source/channel junction, physical thickness of the TMD layer and the gate oxide, respectively.

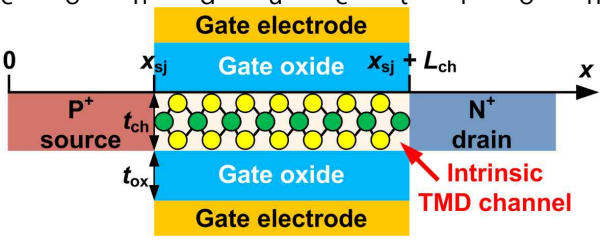

Fig. 1. Schematic of TMD-based DG TFETs.

According to [11], the valence and conduction band profiles from source to drain for a TFET device can be described as

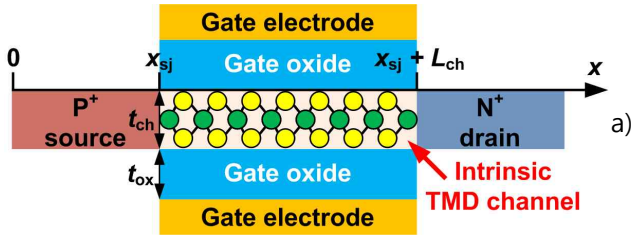

Fig. 1. Schematic of TMD-based DG TFETs.

where U_v and U_c are the valence and conduction band profiles, respectively. In (1a), U_s, U_{ch} and U_d are valence band energy levels in the source, channel and drain, respectively, and determined as

$$U_s = 0, \tag{2a}$$

$$U_{ch} = U_s - E_g/2 - \Delta E_s - q\left(V_g - V_{fb}\right), \tag{2b}$$

$$U_d = U_s - E_g - \Delta E_s - \Delta E_d - qV_d, \tag{2c}$$

where E_g is the direct band gap of the TMD material, q is elementary charge, V_g is the gate voltage, V_d is the drain voltage and V_{fb} is the flat band voltage. ΔE_s and ΔE_d represent $U_s - \mu_s$ and $\mu_d - (U_d + E_g)$, respectively, where μ_s and μ_d are the Fermi levels of the source and drain, respectively. Considering that the 2-D density of states (DOS) is constant, ΔE_s and ΔE_d can be found analytically by solving

$$\begin{aligned} n_s &= \int_{-\infty}^{U_s} D_v\left(1 - f_s\left(E, \mu_s\right)\right) \\ &= \frac{g_s g_v m_h}{2\pi\hbar^2}\left(kT\ln\left(1+\exp\left(\frac{-\Delta E_s}{kT}\right)\right)+\Delta E_s\right), \end{aligned} \tag{3a}$$

$$\begin{aligned} n_d &= \int_{U_d+E_g}^{\infty} D_c f_d\left(E, \mu_d\right) \\ &= \frac{g_s g_v m_e}{2\pi\hbar^2}\left(kT\ln\left(1+\exp\left(\frac{-\Delta E_d}{kT}\right)\right)+\Delta E_d\right), \end{aligned} \tag{3b}$$

where n_s and n_d are 2-D doping densities of the source and drain, respectively, D_v and D_c are constant 2-D DOS of the valence band and conduction band, respectively, f_s and f_d are the Fermi-Dirac distributions of the source and drain, respectively, g_s = 2 and g_v = 2 are the spin and valley degeneracy factors [12], respectively, m_e and m_h are electron and hole effective masses, respectively, $\hbar$ is the Dirac constant, k is the Boltzmann constant and T is lattice temperature.

$\lambda_{eff,s}$ and $\lambda_{eff,d}$ in (1a) are the effective screening length (reciprocal potential decay rate) at the source/channel and channel/drain junction, respectively, and equal to

$$\lambda_{eff,s} = \frac{1}{6}\left(W_{d,s} + \lambda_{ch}\right), \tag{4a}$$

$$\lambda_{eff,d} = \frac{1}{6}\left(W_{d,d} + \lambda_{ch}\right), \tag{4b}$$

where $W_{d,s}$ and $W_{d,d}$ are depletion widths at the source/channel and the channel/drain junction, respectively. In the case of DG FETs, λ_{ch} is given by [13]

$$\lambda_{ch} = \sqrt{\frac{\varepsilon_{ch}}{2\varepsilon_{ox}}\left(1+\frac{\varepsilon_{ox}t_{ch}}{4\varepsilon_{ch}t_{ox}}\right)t_{ch}t_{ox}}, \tag{5}$$

where ε_{ch} and ε_{ox} are permittivites of the TMD layer and gate oxide, respectively. L_{eff} in (1a) is the effective channel length and expressed as

$$L_{eff} = L_{ch} + \left(W_{d,s} - \lambda_{ch}\right)/2 + \left(W_{d,d} - \lambda_{ch}\right)/2. \tag{6}$$

Therefore, when device parameters (n_s, n_d, t_{ch}, t_{ox}, ε_{ch}, ε_{ox}) and bias conditions (V_g, V_d) are confirmed, U_v and U_c of TMD-based DG TFETs can be expressed as continuous functions of x by using (1) ~ (6).

The tunneling probability (T_{tun}) based on the WKB approximation is given by

$$T_{tun} = \exp\left(-2\int_{x_i}^{x_f} dx k_{img}\left(E = E_x - U_v\right)\right), \tag{7}$$

where E_x is the energy of the incoming electron along the transport direction x and k_{img} is the imaginary wave vector in the presence of the tunneling barrier. Neglecting the spin-orbit interaction, the effective two-band Hamiltonian of monolayer TMD materials has the form [14]

$$H = \begin{pmatrix} E_g + \dfrac{\hbar^2|\mathbf{k}|^2(\alpha+\beta)}{4m_0} & ta_0\left(\tau k_x - ik_y\right) \\ ta_0\left(\tau k_x + ik_y\right) & \dfrac{\hbar^2|\mathbf{k}|^2(\alpha-\beta)}{4m_0} \end{pmatrix}, \tag{8}$$

where $\mathbf{k}$ = (k_x, k_y) is the 2-D wave vector, m_0 is the free electron mass, t is the hopping integral, a_0 is the lattice constant, τ = ±1 is the valley parameter for K (+1) and K′ (–1). α and β represent m_0/m_- and $m_0/m_+ - 4m_0v^2/E_g$, respectively, where $m_\pm = m_e m_h/(m_h \pm m_e)$ and $v = ta_0/\hbar$. Thus, the secular equation of (8) is given by

$$\left(E_g+\frac{\hbar^2|\mathbf{k}|^2(\alpha+\beta)}{4m_0}-E\right)\left(\frac{\hbar^2|\mathbf{k}|^2(\alpha-\beta)}{4m_0}-E\right)=(ta_0)^2|\mathbf{k}|^2. \quad (9)$$

After some algebraic manipulation, k_{img} = Im (|**k**|) can be analytically expressed as

$$k_{img}=\sqrt{\frac{E(E_g-E)}{\hbar^2(\alpha-\beta)E+\hbar^2\alpha E}}, \quad (10)$$

when 0< E < E_g.

x_i and x_f in (7) are the initial and final positions of the tunneling in real space, respectively, and can be obtained by satisfying the condition $U_v(x_i)$ = $U_c(x_f)$ = E_x as follows:

$$x_i=\lambda_{eff,s}\ln\left[\frac{\sqrt{h_1^2(E_x)+h_2(E_x)}+h_1(E_x)}{2(E_x-U_d)}\right], \quad (11a)$$

where

$$x_f=\lambda_{eff,s}\ln\left[\frac{\sqrt{h_3^2(E_x)+h_4(E_x)}+h_3(E_x)}{2(E_x-U_d+E_g)}\right], \quad (11b)$$

Therefore, by putting (10), (11a) and (11b) into (7), T_{tun} can be expressed as a function of E_x.

Finally, by using the Landauer formula, the 2-D band-to-band tunneling current per unit width (I_d) can be described as [15]

(12a)

where ΔE is the tunneling window given by U_s – (U_d + E_g). It should be noted that (13) is not analytically integrable. However, numerical integrations of (13) can be performed simply and efficiently. Thus, mathematical approximations for simplifying (13) will not be presented in this paper. In Section III, the numerical evaluation of (13) will be validated by using the NEGF-based quantum transport simulation.

(12b)

(12c)

(12d)

(13)

III. RESULTS AND DISCUSSION

In order to verify the proposed semi-analytical model, sp^3d^5 tight-binding NEGF-based simulation is performed by using the EDISON nanophysics simulator in the case of the monolayer MoS_2-based DG TFET [16], [17]. Spin-orbit interaction is not included because its influence on the band-to-band tunneling current is not significant [18]. The structure of MoS_2 channel in transport direction is assumed to be zigzag. Device parameters are summarized in Table 1.

Device parameters	value
Gate oxide thickness (t_{ox})	1 nm
Channel permittivity (ε_{ch})	4.8
Gate oxide permittivity (ε_{ox})	3.9
Channel length (L_{ch})	5 nm
Source doping concentration (n_s/t_{ch})	10^{20} cm^{-3}
Drain doping concentration (n_d/t_{ch})	10^{20} cm^{-3}

Table. 1. Summary of device parameters for the semi-analytical model and NEGF simulation.

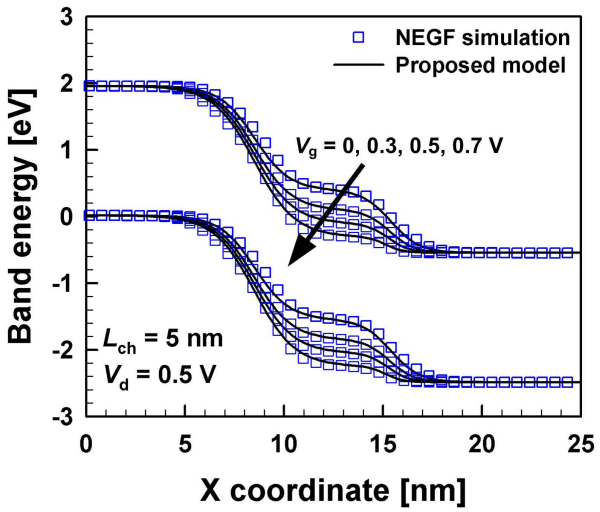

Fig. 2. Modeled and simulated energy band profiles of the 5-nm MoS_2-based DG TFET for V_g = 0, 0.3, 0.5 and 0.7 V

Fig. 2 shows modeled and simulated energy band profiles of the 5-nm monolayer MoS_2-based DG TFET for V_g = 0, 0.3, 0.5 and 0.7 V. It is clearly demonstrated that (1a) and (1b) can reproduce the energy band profiles obtained through NEGF simulations with good

accuracy. As shown in Fig. 2, the monolayer MoS_2-based DG TFET has steep junction band profile at the source/channel junction despite of

extremely-scaled L_{ch} of 5 nm. It is because of thin t_{ch} (7 Å) and low ε_{ox} (4.8) of MoS_2 channel layer, which makes the λ_{ch} and accordingly λ_{eff} smaller. Fig. 3 compares the transfer curves of the 5-nm MoS_2-based DG TFET calculated from the proposed model and from the previous model (Ma's model, [10]) with the tight-binding NEGF simulation results. It shows that the proposed modeling results

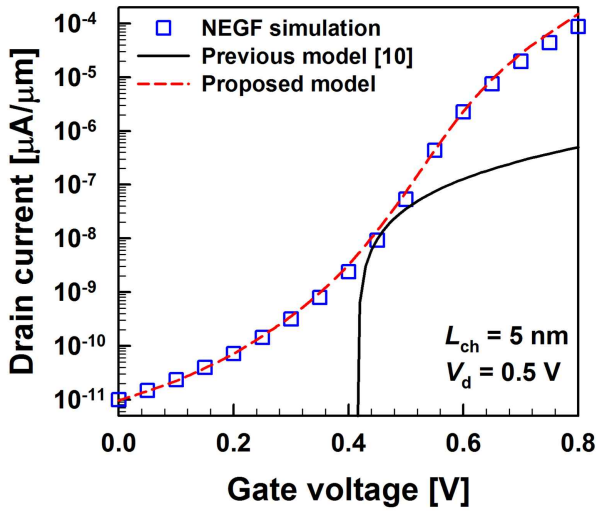

Fig. 3. Comparison of transfer characteristics of the 5-nm MoS_2-based DG TFET obtained from the proposed model, previous model [10] and the tight-binding NEGF simulation.

match the NEGF simulation results well, while the previous modeling results underestimate the 2-D band-to-band tunneling current significantly. It is mainly due to the T_{tun} in [10] is calculated by assuming the linear energy band profile at the tunneling junction and the parabolic band structure, so-called Kane-Sze model [3], [11]. Kane-Sze model is frequently used to evaluate the band-to-band tunneling current of TFET devices due to its simplicity. However, as shown in this work, the accurate transfer characteristics of ultra-scaled TMD-based TFETs can hardly be obtained by using the Kane-Sze model. Therefore, the proposed model in this paper will be useful for investigating the realistic performance of TMD-based TFETs.

IV. CONCLUSION

In this paper, the analytical model of TMD-based DG TFETs is proposed. The proposed model is based on the 2-D Landauer formula, WKB approximation with nonlinear, continuous energy band profile and two-band effective Hamiltonian. The modeling results are in good agreement with tight-binding NEGF simulation results in the case of the 5-nm monolayer MoS_2-based DG TFET. Thus, the proposed model can give the accurate prediction of the performance of TMD-based TFETs as well as the insight on the underlying physics of the 2-D band-to-band tunneling.

ACKNOWLEDGEMENT

This research was supported by the EDISON Program through the National Research Foundation of Korea (NRF) funded by the Ministry of Science, ICT & Future Planning (2012M3C1A6035302)

REFERENCES

[1] M. Ionescu and H. Riel, "Tunnel field-effect transistors as energy-efficient electronic switches," *Nature*, vol. 479, no. 7373, pp. 329-337, Nov. 2011.

[2] W. Y. Choi, B. G. Park, J. D. Lee, and T. J. K. Liu, "Tunneling field-effect transistors (TFETs) with subthreshold swing (SS) less than 60 mV/dec," *IEEE Electron Device Lett.*, vol. 28, no. 8, pp. 743-745, Aug. 2007.

[3] A. C. Seabaugh and Q. Zhang, "Low-voltage tunnel transistors for beyond CMOS logic," *Proc. IEEE*, vol. 98, no. 12, pp. 2095-2110, Dec. 2010.

[4] S. Agarwal and E. Yablonovitch, "Band-edge steepness obtained from Esaki/backward diode current–voltage characteristics," *IEEE Trans. Electron Devices*, vol. 61, no. 5, pp. 1488-1493, May. 2014.

[5] S. Agarwal and E. Yablonovitch, "Designing a Low Voltage, High Current Tunneling Transistor," in CMOS and Beyond: Logic Switches for Terascale Integrated Circuits, T.-J. K. Liu and K. Kuhn, Eds., ed: Cambridge University Press, 2014.

[6] R. H. Yan, A. Ourmazd, and K. F. Lee, "Scaling the Si MOSFET: from bulk to SOI to bulk" *IEEE Trans. Electron Devices*, vol. 39, no. 7, pp. 1704-1710, Jul. 1992.

[7] H. Ilatikhameneh, Y. Tan, B. Novakovic, G. Klimeck, R. Rahman, and J. Appenzeller, "Tunnel field-effect transistors in 2-D transition metal dichalcogenide materials," *IEEE J. Exploratory Solid-State Comput. Devices and Circuits*, vol. 1, pp. 12-18. Feb. 2015.

[8] R. K. Ghosh and S. Mahapatra, " Monolayer Transition Metal Dichalcogenide Channel-Based Tunnel Transistor," *IEEE J.*

Electron Devices Soc., vol. 1, no. 10, pp. 175-180, Oct. 2013.
[9] C. Gong, H. Zhang, W. Wang, L. Colombo, R. M. Wallace, and K. Cho "Band alignment of two-dimensional transition metal dichalcogenides: Application in tunnel field effect transistors," *Appl. Phys. Lett.*, vol. 103, no. 5, pp. 053513, Aug. 2013.
[10] N. Ma and D. Jena, "Interband tunneling in two-dimensional crystal semiconductors," *Appl. Phys. Lett.*, vol. 102, no. 13, pp. 132102, Apr. 2013.
[11] R. B. Salazar, H. Ilatikhameneh, R. Rahman, G. Klimeck, and J. Appenzeller, "A predictive analytic model for high-performance tunneling field-effect transistors approaching non-equilibrium Green's function simulations," *J. Appl. Physics*, vol. 118, no. 16, pp. 164305, Oct. 2015.
[12] J. Hong, C. Lee, J. S. Park, J. S. and J. H. Shim, "Control of Valley Degeneracy in MoS2 by Layer Thickness and Electric Field and Its Effect on Thermoelectric Properties," Phys. Rev. B, vol. 93, no. 3, pp. 035445, Jan. 2016.
[13] L. Liu, D. Mohata, and S. Datta, "Scaling length theory of double-gate interband tunnel field-effect transistors," IEEE Trans. *Electron Devices*, vol. 59, no. 4, pp. 902-908, Apr. 2012.
[14] H. Rostami, A. G. Moghaddam, and R. Asgari, "Effective lattice Hamiltonian for monolayer MoS_2: Tailoring electronic structure with perpendicular electric and magnetic fields," *Phys. Rev. B*, vol. 88, no. 8, pp. 085440, Aug. 2013.
[15] S. Agarwal and E. Yablonovitch, "Using dimensionality to achieve a sharp tunneling FET (TFET) turn-on," in *Proc. 69th Annu. Device Res. Conf. (DRC)*, Santa Barbara, CA, USA, 2011, pp. 199–200.
[16] V. Mishra, S. Smith, L. Liu, F. Zahid, Y. Zhu, H. Guo, and S. Salahuddin, "Screening in Ultrashort (5 nm) Channel MoS_2 Transistors: A Full-Band Quantum Transport Study," *IEEE Trans. Electron Devices*, vol. 62, no. 8, pp. 2457-2463, Aug. 2015.
[17] *EDISON Nanophysics Simulator*, National Institude of Supercomputing and Networking (NISN), Korean Institude of Science and Technology Information (KISTI) [Online]. Available: http://nano.edison.re.kr/
[18] M. Luisier, G. Klimeck, "Atomistic full-band design study of InAs band-to-band tunneling field-effect transistors," *IEEE Electron Device Lett.*, vol. 30, no. 6, pp. 602-604, Jun. 2009.